Volume 17 Number 24 1989 Nucleic Acids Research

High resolution footprinting of *Eco*RI and distamycin with $Rh(phi)_2(bpy)^{3+}$, a new photofootprinting reagent

Kiyoshi Uchida+, Anna Marie Pyle§, Takashi Morii$^{\phi}$ and Jacqueline K.Barton*$^{\phi}$

Department of Chemistry, Columbia University, New York, NY 10027, USA

Received September 18, 1989; Revised and Accepted November 8, 1989

ABSTRACT

The complex bis(phenanthrenequinone diimine)(bipyridyl)rhodium(III), $Rh(phi)_2(bpy)^{3+}$, cleaves DNA efficiently in a sequence-neutral fashion upon photoactivation so as to provide a novel, high resolution, chemical photofootprinting reagent. Photofootprinting of two crystallographically characterized DNA-binding agents, distamycin, a small natural product which binds to DNA in the minor groove, and the endonuclease EcoRI, which binds in the major groove, gave respectively a 5−7 base pair footprint for the drug at its A_6 binding site and a 10−12 base pair footprint for the enzyme centered at its recognition site (5'-GAATTC-3'). Both footprints agree closely with the crystallographic results. The photocleavage reaction can be performed using either a high intensity lamp or, conveniently, a simple transilluminator box, and the photoreaction is not inhibited by moderate concentrations of reagents which are sometimes required for examining interactions of molecules with DNA. When compared with other popular footprinting agents, the rhodium complex shows a number of distinct advantages: sequence-neutrality, high resolution, ability to footprint major as well as minor groove-binding ligands, applicability in the presence of additives such as Mg^{2+} or glycerol, ease of handling, and a sharply footprinted pattern. Light activated footprinting reactions furthermore offer the possibility of examining DNA-binding interactions with time resolution and within the cell.

INTRODUCTION

The technique of DNA footprinting has been used extensively to observe the site-specific binding of proteins, peptides, and drugs to DNA (1−4). Using a variety of chemical and enzymatic footprinting agents, it has been possible to determine the relative binding site sizes and locations for a large variety of DNA-binding proteins. Subtle molecular interactions between DNA and transcription factors, repressors, and other constituents of the transcriptional apparatus are being actively explored using DNA footprinting (5).

Given the power of this methodology, extensive efforts to find new, high resolution reagents for footprinting are underway. The most popular and the original footprinting reagent is DNase I, a large nuclease which cleaves with some preference for sequences of intermediate groove widths (6). This level of sequence-neutrality is sufficient for determining the binding sites of large DNA binding proteins. However, small peptides or proteins which bind to sequences insensitive to attack by DNase I can be difficult to visualize. Many synthetic footprinting reagents such as $Cu(phen)_2^+$ and metalloporphyrins share this inherent problem (7,8). In order to examine DNA binding interactions at higher resolution, many workers have turned to MPE-Fe(II), the first synthetic footprinting reagent and a remarkable tool with respect to its sequence neutrality. An intercalating dye tethered to an $Fe(EDTA)^{2-}$ moiety, MPE-Fe(II) has been useful in elucidating the binding sites and sizes of small natural products as well as proteins (9−12). More recently, the clever

application to footprinting of $Fe(EDTA)^{2-}$ itself, without a tethered DNA-binding moiety, has been made (3,13). Both for $Fe(EDTA)^{2-}$ and MPE-Fe(II), cleavage results from the diffusion to the DNA helix of hydroxyl radicals, generated in the presence of peroxide and a reducing agent (3,9,13). $Fe(EDTA)^{2-}$, which as an anionic species generates the radicals far from the DNA surface, also shows a high level of sequence neutrality, but since the radical generator does not bind to the DNA, high concentrations of reagents are required. Additionally a drawback with respect to both complexes has been their sensitivity to the presence of various common additives, such as glycerol or Mg^{2+}, and their requirements for high concentrations of chemical activators.

Some techniques of photofootprinting have also been developed. An advantage of this method is that the activation of the DNA cleavage reaction is controlled by light, eliminating the need for adding other chemicals to the protein solution. These techniques include ultraviolet footprinting (14), photofootprinting in the presence of uranyl salts (15), and that in the presence of psoralen or its analogs (16). Ultraviolet light photofootprinting has been applied *in vivo* as well as *in vitro*. This technique requires chemical treatment after the photocleavage reaction, however, and the results obtained are sometimes complicated because of differential enhancements due to DNA-protein crosslinking. The second technique, using uranyl salts, shows excellent sequence neutrality but high concentrations of the uranyl salts are required, which may perturb the protein interactions with the DNA or the DNA structure itself. The cleavage pattern with psoralen shows sequence preferences (16). Owing to these difficulties, despite the inherent advantages of light activation, these photofootprinting reagents have not been widely applied.

Recently, coordinatively saturated phenanthrenequinone diimine complexes of rhodium(III) have been reported to cleave DNA efficiently upon irradiation with long-wavelength ultraviolet light (17). Photocleavage with $Rh(phi)_2(bpy)^{3+}$ yields sharp, sequence-neutral cleavage of linear DNA fragments. The addition of free metal ions, chelators, or oxidizing agents is not necessary in this system because the $Rh(phi)_2(bpy)^{3+}$ complex is fully assembled and requires activation only by light. The structure of $Rh(phi)_2(bpy)^{3+}$ is schematically illustrated below.

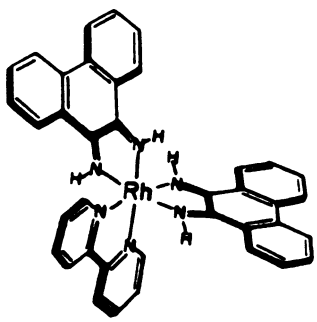

Here we report the development of $Rh(phi)_2(bpy)^{3+}$ as a high-resolution photofootprinting reagent which successfully maps the precise binding locations and site sizes of distamycin-A and the restriction endonuclease EcoRI. This is the first report of a footprint for EcoRI by a synthetic footprinting reagent and the first example of a footprint which reflects the proper site size (18). $Rh(phi)_2(bpy)^{3+}$ is able to detect both EcoRI bound in the major

groove of DNA and the small peptide distamycin, bound in the minor groove. Footprinting with $Rh(phi)_2(bpy)^{3+}$ is not inhibited by moderate concentrations of salts, EDTA, glycerol, or reducing agents, many of which are sometimes necessary to obtain a native interaction of DNA with protein. The complex is easy to handle, being very stable under ordinary conditions and requiring no complicated reaction conditions. Activation with low energy light from a lamp or transilluminator permits excellent experimental control over $Rh(phi)_2(bpy)^{3+}$ footprinting, an absolute requirement for application *in vivo*.

EXPERIMENTAL

Materials

$[Rh(phi)_2(bpy)]Cl_3$ was synthesized as described previously (17) and MPE was kindly provided by Prof. P.B. Dervan. Distamycin A, alkaline phosphatase, bovine serum albumin, and 2,9-dimethyl-1,10-phenanthroline were obtained from Sigma; lyophilized *Eco*R I, *Hin*dIII, *Pvu* II, terminal deoxynucleotidyl transferase and T4 polynucleotide kinase from BRL; DNase I from Boehringer Mannheim; dithiothreitol, 3-mercaptopropionic acid, and 1,10-phenanthroline from Aldrich; and α-^{32}P-3′-dATP and γ-^{32}P-ATP from NEN. Tris-acetate buffer for irradiations with $Rh(phi)_2(bpy)^{3+}$ contained the following unless specified otherwise: 50 mM tris, 20 mM sodium acetate, 18 mM NaCl, pH 7. Loading buffer for electrophoresis on a denaturing polyacrylamide gel contained 80 % formamide, 50 mM tris borate buffer (pH 8), 0.1 % xylene cyanol, 0.1 % bromophenol blue, 0.1 N NaOH, and 1 mM EDTA. Polyacrylamide Gel-Mix 8 from BRL was used for pouring denaturing polyacrylamide gels.

Preparation of Labeled DNA fragment:

Plasmid pJT18-T6 was obtained by inserting an 18 base pair oligonucleotide (5′-ATATGCAAAAAAGCATAT-3′) by blunt-end ligation into the *Sma* I site of plasmid pUC 18 and amplifying in *E. coli* (JM109) cells by culture. The plasmid was isolated according to methods published in the literature (19). The plasmid thus obtained was first digested with restriction enzyme *Hin*d III and purified by ethanol precipitation. To obtain the 3′ end-labeled fragment, ^{32}P-α-3′-dATP and terminal deoxynucleotidyl transferase were reacted with linearized DNA. This was followed by a second digestion with *Pvu* II, yielding a 245 bp DNA fragment containing the insert which was purified on a 5% polyacrylamide gel and isolated by subsequent electrophoretic elution. The DNA fragment was then ethanol precipitated in the presence of sodium acetate and washed with EtOH. After lyophilization, the DNA fragment was dissolved in 1/10 dilution tris-acetate buffer containing 0.1mM EDTA for use or storage at 4°C. To obtain the 5′ end-labeled fragment, linearized DNA was treated with alkaline phosphatase and labeled with γ-^{32}P-ATP in the presence of polynucleotide kinase. Fragment isolation and purification were performed as described for the 3′ end-labeled fragment. If ^{32}P-labeled samples were stored for appreciable time, some background damage was evident in the autoradiograms of the unreacted fragment.

DNA Cleavage by $Rh(phi)_2(bpy)^{3+}$

A typical procedure for carrying out DNA photocleavage with $Rh(phi)_2(bpy)^{3+}$ in the absence of any other DNA-binding molecule was as follows: 50 μl of a reaction mixture containing ^{32}P-end labeled DNA fragment (5 μM bp and approx 30,000 cpm, concentration adjusted with calf thymus carrier DNA), and 5 μM $[Rh(phi)_2(bpy)]Cl_3$ (ϵ_{350} = 23,600 $M^{-1}cm^{-1}$) in tris-acetate buffer was added to a 1.7 ml siliconized polypropylene tube. Open reaction tubes were fixed such that the reaction mixture was

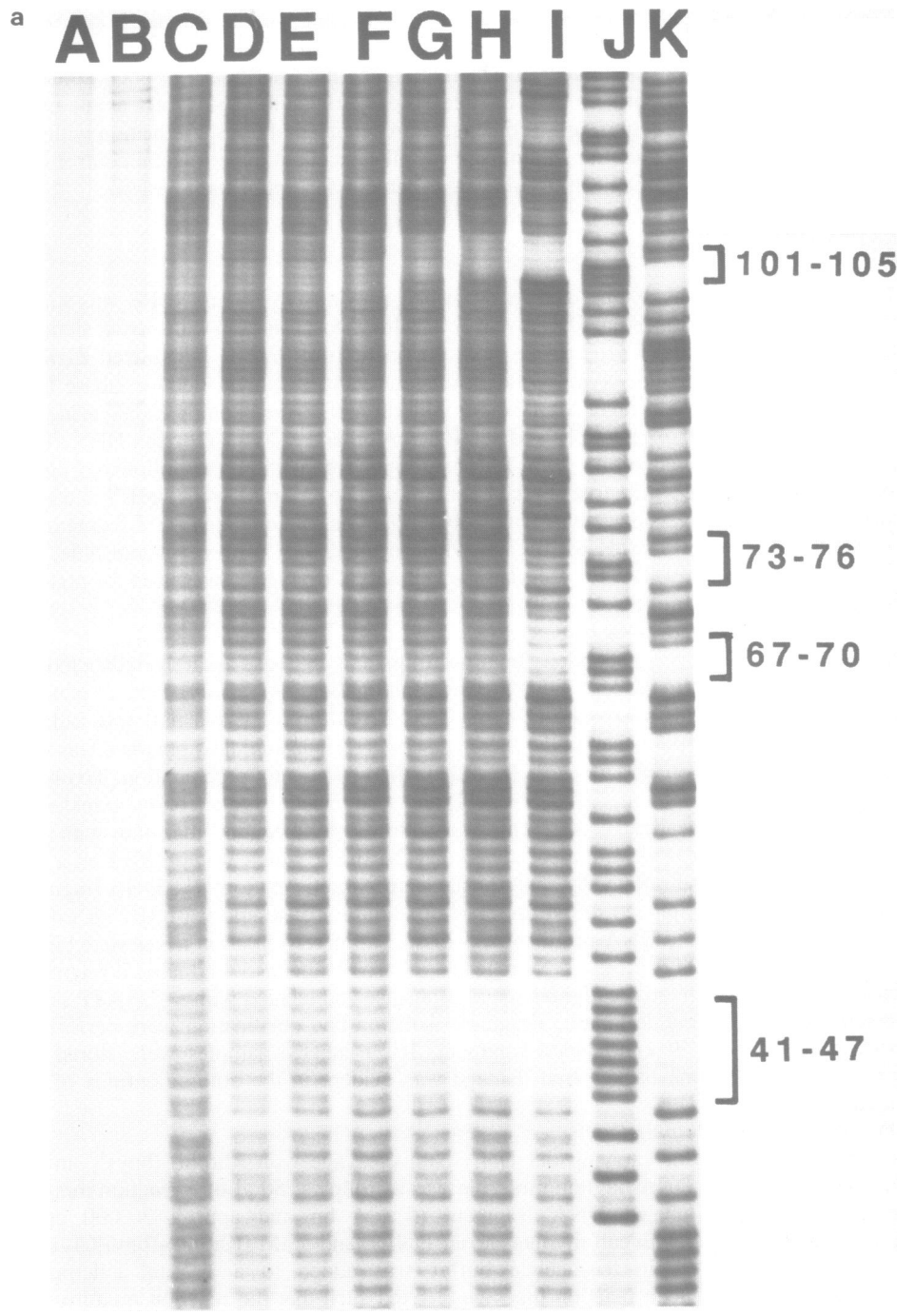
a
A B C D E F G H I J K
101-105
73-76
67-70
41-47

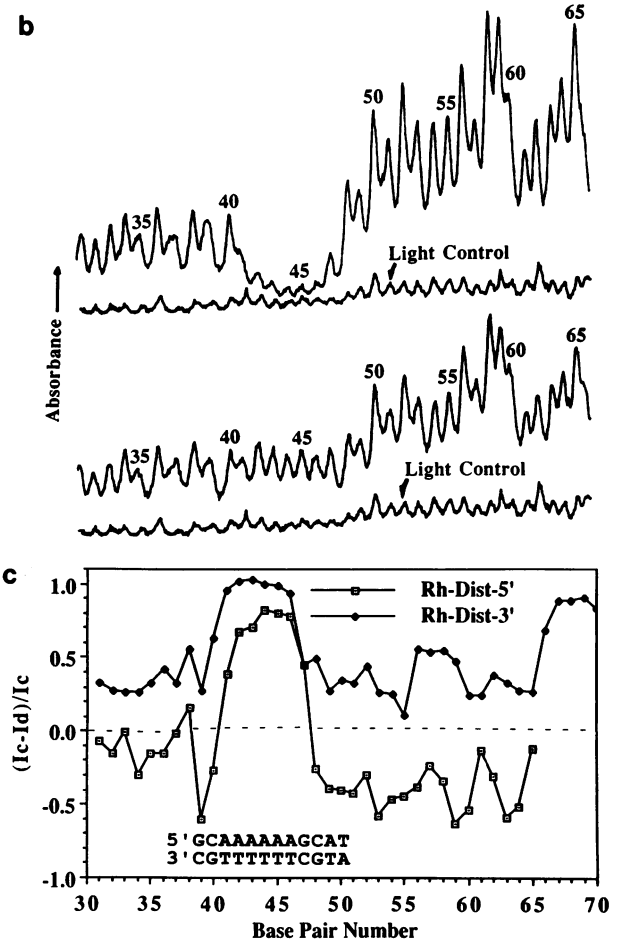

Figure 1. (a). $Rh(phi)_2(bpy)^{3+}$ footprinting of distamycin. Lanes A and B: dark and light controls, respectively. Lanes C and D: in the absence of distamycin (C without 90 °C treatment after cleavage reaction); E, F, G, H, and I: in the presence of 0.125, 0.25, 1.25, 2.5, and 12.5 μM distamycin, respectively, using 5′-end-labeled fragment and 7 min irradiation with a Hg/Xe lamp. Lanes J and K: Maxam-Gilbert A+G and T+C reactions, respectively. The footprinted regions are marked with brackets and numbers. For better resolution of the footprints, the higher molecular weight region of the gel is not shown.

(b). Densitometer scans of $Rh(phi)_2(bpy)^{3+}$ footprinting in the presence of distamycin (top, data from lane I of Fig 1a) and in the absence of distamycin (bottom, data from lane D of Fig. 1a). Traces of light control and base pair numbers are given in each scan for reference.

(c). Values of (Ic−Id)/Ic for footprinting of distamycin are plotted against base pair numbers for both 5′- and 3′-end-labeled strands. Data were taken from Figure 1A. The sequence at the footprinted region is inset.

directly in the focal point of a 1000 W Hg/Xe lamp beam focused and filtered with a monochrometer (Oriel model 77250) and a glass filter to eliminate the light below 300 nm. Samples were irradiated at 310 nm for approximately 5 minutes. After irradiation, 1 μl of ~3 μg/μl calf thymus DNA and 25 μl of 7.5 M ammonium acetate were added to the reaction mixture, which was then heated at 90 °C for 2 min and precipitated by

addition of 150 μl EtOH. We have found this melting procedure to give sharper cleavage patterns on electrophoresis, presumably as a result of fully dissociating the metal complex. The DNA pellet was rinsed with 70% ethanol and then lyophilized. After addition of 2.5 μl loading buffer, the samples were electrophoresed on an 8% denaturing polyacrylamide gel. In all photocleavage experiments two control lanes were included: the DNA control, which was simply the labeled fragment without metal or light activation, and the light control, which corresponded to the labeled fragment irradiated in the absence of metal

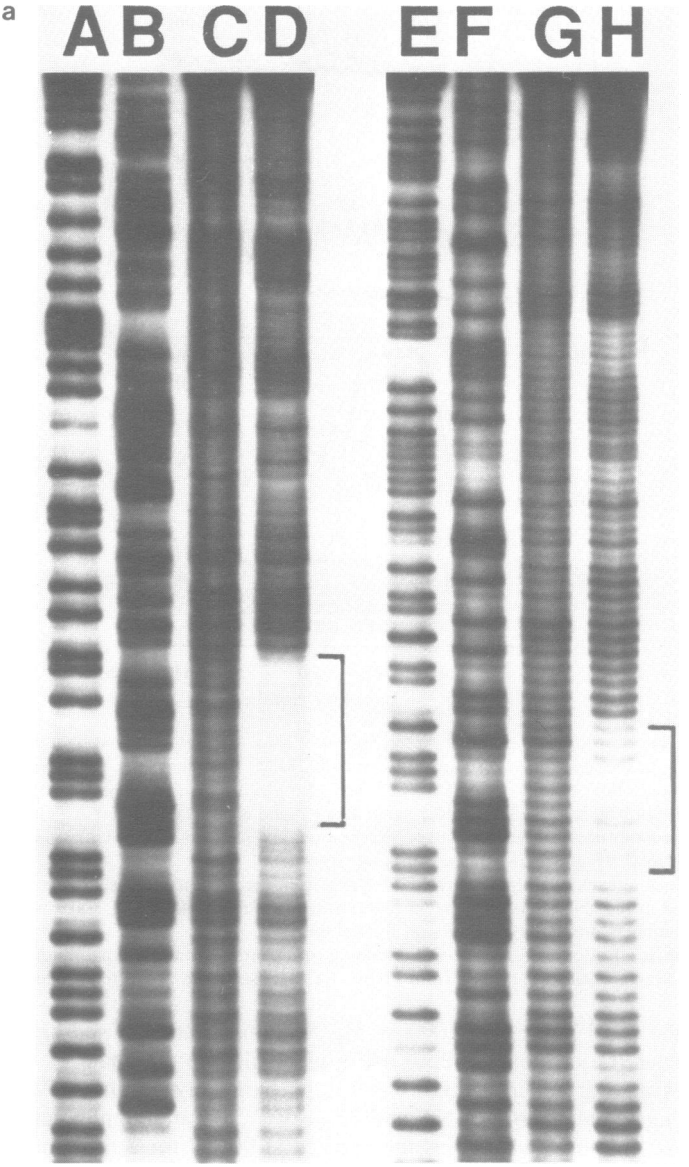

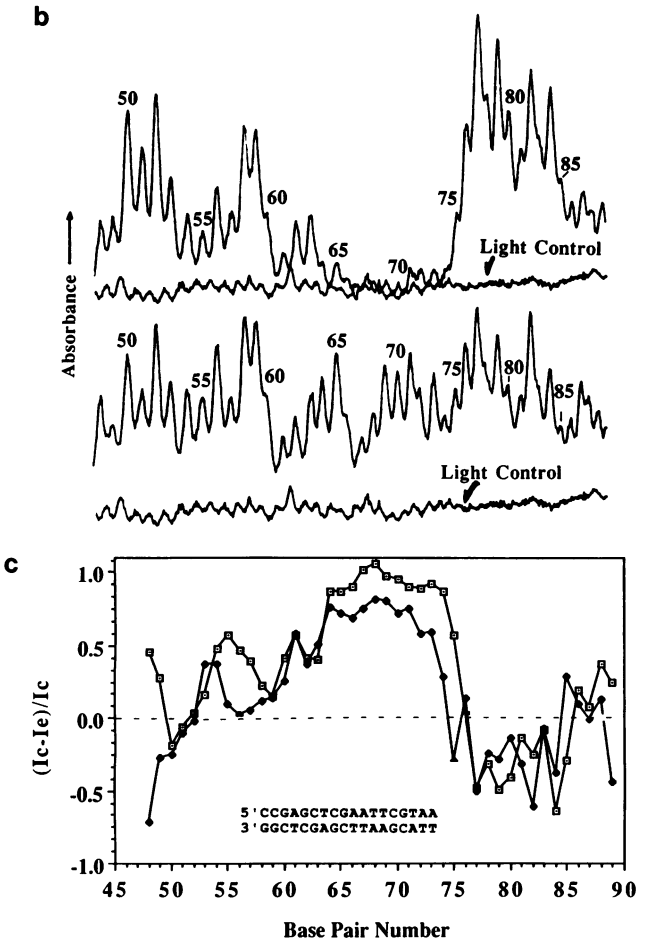

Figure 2 (a) $Rh(phi)_2(bpy)^{3+}$ footprinting of *EcoRI*. Lanes A−D on 5′-end-labeled fragment and E−H on 3′-end-labeled fragment. Lanes C and G: $Rh(phi)_2(bpy)^{3+}$ cleavage in the absence of *EcoRI*. D and H: cleavage in the presence of *Eco*RI (60 units for lane D and 240 units for lane H) after 6 min irradiation with a Hg/Xe lamp. Lanes A and E: Maxam-Gilbert A+G reaction. Lanes B and F: T+C reaction. The strongest footprinted region (64−75 on the 5′-end-labeled strand and 64−73 on the 3′-end-labeled strand) is indicated by brackets. For better resolution of the footprints, the higher molecular weight region of the gel is not shown.

(b). Densitometer scans of $Rh(phi)_2(bpy)^{3+}$ footprinting of *Eco*RI on 5′ end-labeled fragment in the presence (top) and absence (bottom) of the endonuclease, together with the light control lane. Base pair numbers are also given.

(c). Values of (Ic−Ie)/Ic are plotted against base pair number for 5′-and 3′-end-labeled strands.

complex. Inspection of the DNA control gave an assessment of the background damage from labeling and/or storage, and inspection of the light control gave an assessment of the extent of photodamage (usually negligible).

$Rh(phi)_2(bpy)^{3+}$ Footprinting of Distamycin and EcoRI

Distamycin-A was dissolved in deionized water and the concentration of stock solution was determined optically, using $\epsilon_{302\,nm} = 3.4\times10^4\,M^{-1}cm^{-1}$ (20). Final reaction mixtures

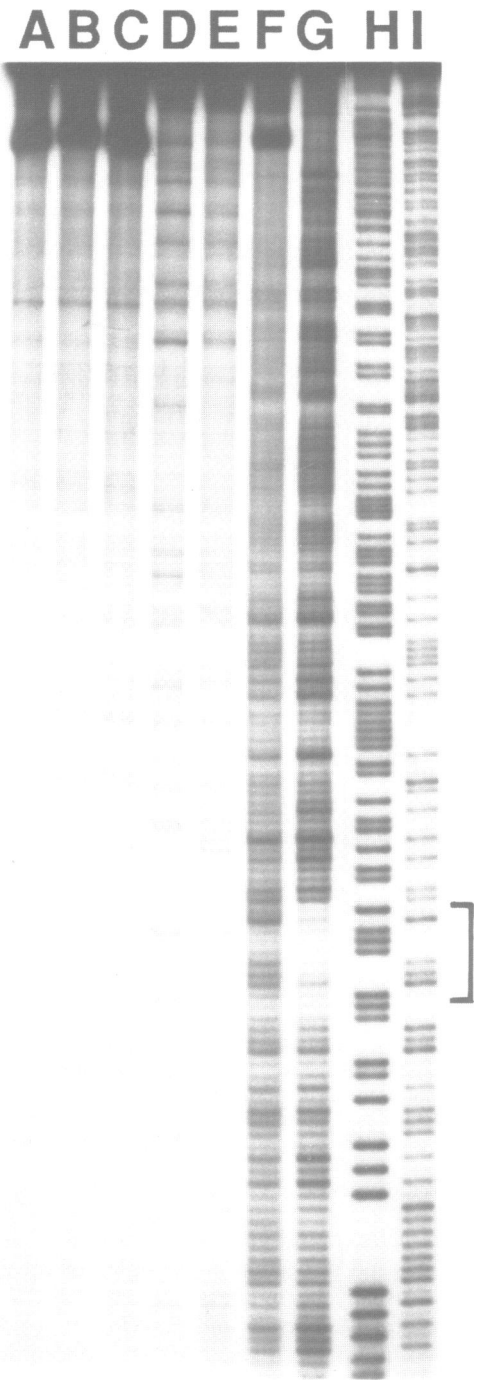
A B C D E F G H I

in tris-actetate buffer contained 0.125−25 μM distamycin, 25 μM bp ^{32}P-end labeled fragment DNA (nucleotide concentration adjusted with calf thymus DNA carrier) and 12.5 μM [Rh(phi)$_2$(bpy)]Cl$_3$. After addition of distamycin to DNA, the solution was allowed to stand at room temperature for 10 minutes before addition of the rhodium complex. This was followed by another 15 minute room temperature incubation before irradiation as described above. For EcoRI footprinting, EcoRI was dissolved to a final concentration of 40 units/μl in tris-acetate buffer containing 0.1 mM calcium chloride and left at 0 °C for 1 hour (One pmole of the endonuclease corresponds to 769 units, by assuming that the turnover number of the enzyme is 4 per hour per dimer (21)). The final reaction mixture in tris-actetate buffer contained 60−360 units of EcoRI, 5 μM bp ^{32}P-end labeled fragment DNA (nucleotide concentration adjusted with pUC18 carrier), 1 mM calcium chloride (necessary to displace traces of Mg^{2+} in the enzyme (18)), and 5 μM Rh(phi)$_2$(bpy)$^{3+}$. DNA and EcoRI were incubated together for 30 minutes, then again for 15 minutes after the addition of Rh(phi)$_2$(bpy)$^{3+}$. Following irradiation, the reaction mixture was ethanol precipitated in the presence of ~4 μg calf thymus DNA, followed by phenol/chloroform extraction, and another ethanol precipitation.

Rh(phi)$_2$(bpy)$^{3+}$ Footprinting of EcoRI Using a Transilluminator

The reaction mixture was prepared as described above. 50 μl irradiation volumes were then placed in 'short tubes' (capless 1.7 ml siliconized polypropylene tubs cut down to small cups approximately 7 mm high and 100 μl in volume, to minimize the distance between reaction mixtures and the UV-light source), which were placed in a pipette-tip rack and irradiated by inverting a UV transilluminator (Spectroline Model # TR302 for visualizing ethidium-stained agarose gels with a broad band of irradiation centered at 302 nm) on top of them. The UV-filter of the transilluminator may be removed to increase light intensity. Samples should be less than 1 cm from the light source and irradiated for 20 min at room temperature. Work-up was the same as described previously.

Footprinting with other reagents

Footprinting reactions for distamycin and EcoRI were conducted using the DNA binding ligands at comparable concentrations to those employed for the rhodium complex (described above), but using cleavage methodologies for DNase I, MPE-Fe(II) and Cu(phen)$_2^+$ according to the literature (1,2,4,9,22). Samples were purified and prepared for electrophoresis as after photocleavage by the rhodium complex; some loss of low molecular weight fragments, after ethanol precipitation, could therefore be discerned in some autoradiographs.

Electrophoresis, Autoradiography, Densitometry and Data Processing

DNA pellets from the footprinting reactions were dissolved in 2.5 μl loading buffer and electrophoresed on an 8% denaturing polyacrylamide gel as described (19). Reaction products were coelectrophoresed with Maxam-Gilbert sequencing reactions (23). After removal from the plates, the gels were dried and subjected to autoradiography (Kodak, X-OMAT^{TM}AR) at room temperature (or −60 °C) without an intensifying screen for 2−20 days. Autoradiographs were scanned on a 2202 Ultra Scan Laser Densitometer

Figure 3 Rh(phi)$_2$(bpy)$^{3+}$ footprinting of *Eco*RI using a transilluminator as light source. Lanes F and G: cleavage by Rh(phi)$_2$(bpy)$^{3+}$ in the absence and presence of EcoRI (296 units), respectively, using 20-min irradiation with the box. Lane A: Intact 245 bp DNA fragment, 3′-end-labeled. Lanes B and C: dark controls in the absence and presence of *Eco*RI, respectively. Lanes D and E: light controls in the absence and presence of *Eco*RI, respectively. Lanes H and I: Maxam-Gilbert A+G and C+T reactions, respectively. The footprinted region between 64−73 is indicated by a bracket.

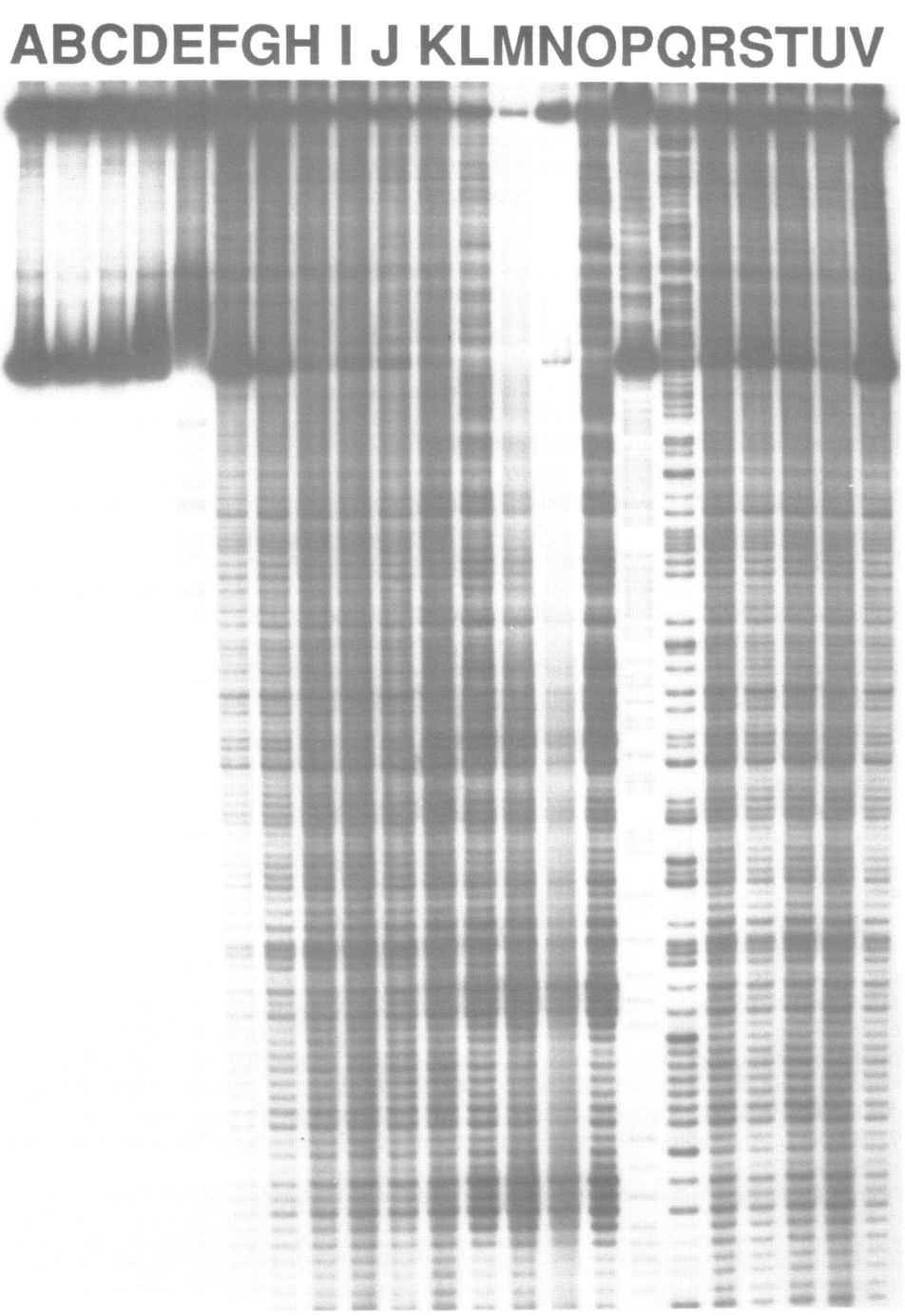
ABCDEFGH I J KLMNOPQRSTUV

(LKB). To obtain the integrated intensity (I) of each peak, the integrated area of the light control or DNA control (for reagents not requiring light activation) was subtracted. The resulting I_d or I_e (corrected integrated intensity in the presence of distamycin or *Eco*RI, respectively) was then subtracted from I_c (the integrated intensity in the absence of distamycin or *Eco*RI) and reported as a normalized ratio. The final value of $(I_c-I_d)/I_c$ or $(I_c-I_e)/I_c$ for a given band was then equal to 1 for complete protection, 0 for the total absence of protection and a negative value for enhanced cleavage in the presence of distamycin or EcoRI.

RESULTS

$Rh(phi)_2(bpy)^{3+}$ Footprinting of Distamycin

Footprinting of distamycin on a 5′-end-labeled DNA fragment is shown in Figure 1a. Brackets denote regions where the DNA is protected from $Rh(phi)_2(bpy)^{3+}$cleavage by distamycin. A clear, sharp footprint is seen at the strong A_6 binding site (41−47 bp) for distamycin and also at weaker distamycin binding sites AATT (67−70), TAAT (73−76), AAATT (101−105), and TTAT (107−110). On the 3′-end-labeled fragment, corresponding results are obtained. At a higher concentration of distamycin (25 μM, drug/base pair ratio = 1) and a lower concentration of the rhodium complex (6.5 μM, rhodium/base pair ratio = 0.26), a weak ATAT site and sites containing three AT base pairs can also be footprinted. Figure 1b shows densitometer traces of $Rh(phi)_2(bpy)^{3+}$ cleavage in the presence and absence of distamycin. Densitometer data were also manipulated as described in *Experimental* to yield Figure 1c, a representation of high resolution footprinting at the A_6 site by $Rh(phi)_2(bpy)^{3+}$ on both strands. For the 5′-end-labeled fragment, 5 bases (42−46) are strongly protected from cleavage and 2 bases (41 and 47) are weakly protected. For the 3′-end-labeled fragment, 6 (41−46) and 1 (40) positions are strongly and weakly protected from cleavage, respectively.

$Rh(phi)_2(bpy)^{3+}$ Footprinting of EcoRI

Figure 2a shows the footprinting of EcoRI by $Rh(phi)_2(bpy)^{3+}$ on 5′-(lanes A−D) and 3′-(lanes E−F) end-labeled fragments. A sharp footprint of the protein is clearly evident. Densitometer scans are shown in Figure 2b for cleavage by $Rh(phi)_2(bpy)^{3+}$ in the presence and absence of EcoRI, and Figure 2c shows the values of $(I_c-I_e)/I_c$ for each band on both 3′ and 5′-end-labeled strands. It is apparent from Figure 2c that the footprinted region about the EcoRI site is 12 bases (64−75) in length on the 5′-end-labeled strand and 10 bases (64−73) on the 3′-end-labeled strand. These footprinted regions are much smaller than those obtained with DNase I (17−18 base pairs) (18) and are in good

Figure 4 Autoradiogram of 3′-end-labeled DNA fragment photocleaved in the presence of $Rh(phi)_2(bpy)^{3+}$ under various conditions. Lanes A−E are controls: A: Intact DNA fragment (no irradiation and no metal complex). B and C: dark controls (room temperature for 10 and 50 min, respectively, in the dark) in the presence of 5 and 15 μM Rh-complex, respectively. D and E: light controls (no Rh-complex) with 10- and 50-min irradiation, respectively, with focused maximum intensity (I_{max}) of a Hg/Xe lamp. Lanes F, G, and H: 15 μM Rh-complex and 1 min, 3 min 20 sec, and 10 min irradiation (I_{max}) , respectively. Lanes I, J, and K: 10, 5, and 2.5 μM, rhodium complex, respectively, and 10 min irradiation (I_{max}). Lanes L, M, and N: 1 μM Rh-complex and 10, 25, and 50 min irradiation (I_{max}), respectively. Lane O: 0.5 μM and 10 min irradiation (I_{max}). Lane R: 5 μM rhodium complex and 10 min irradiation with $I_{max}/2$. Lanes S, T, and U: 5 μM rhodium complex and 10, 25, and 50 min irradiation with $I_{max}/5$, respectively. Lane V: 5μM Rh-complex and 10 min irradiation with $I_{max}/10$. Total DNA concentration was 5μM base pairs. Lanes P and Q were Maxam-Gilbert A+G and T+C reactions, respectively.

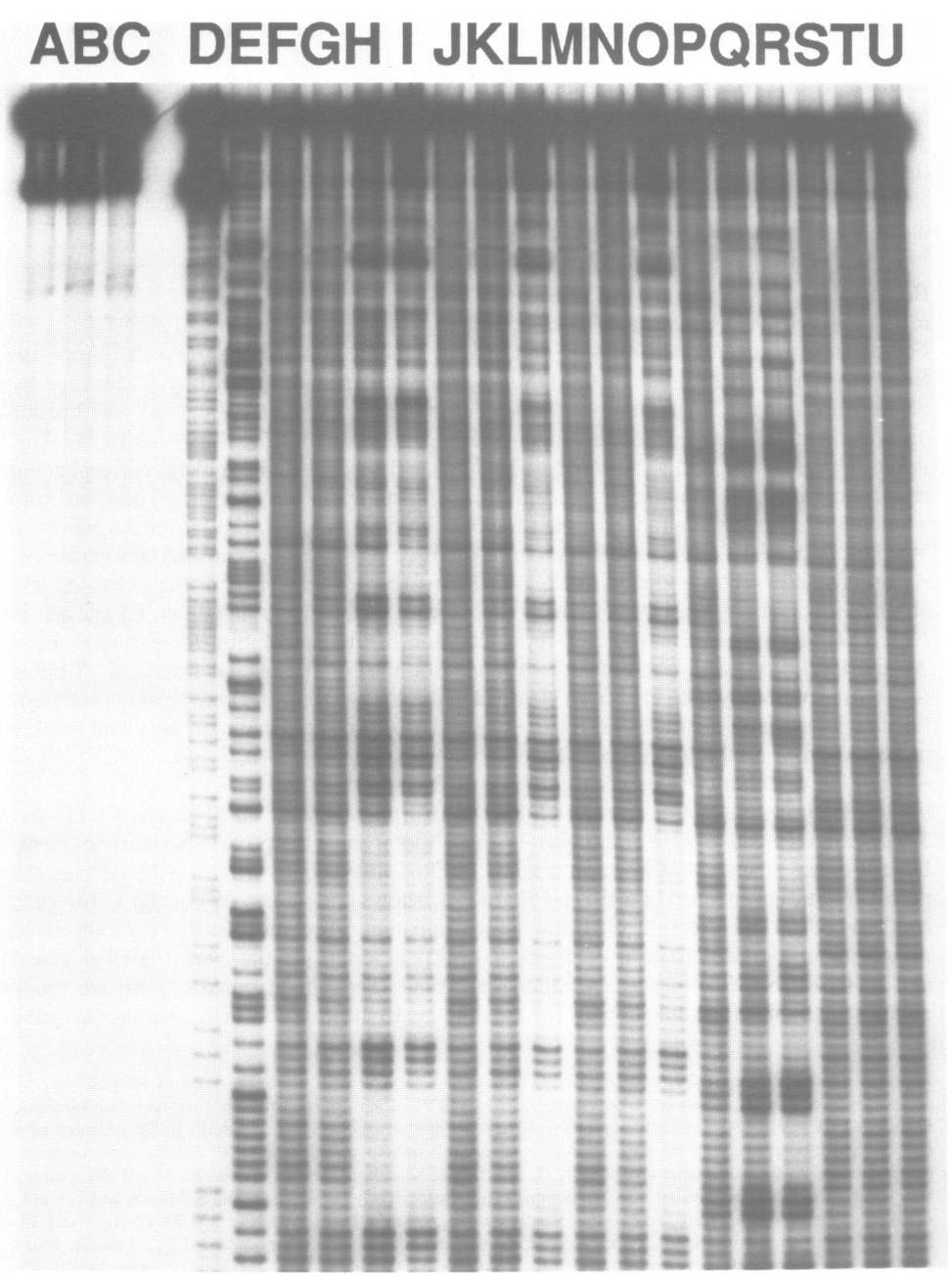
ABC DEFGH I JKLMNOPQRSTU

agreement with the x-ray co-crystallographic data, where the protein is seen to be in contact with the DNA over 10 base pairs (24).

Footprinting experiments were also conducted with $Rh(phi)_2(bpy)^{3+}$ using a transilluminator, commonly found in biology laboratories, as a light source. The footprint of EcoRI obtained by irradiation of $Rh(phi)_2(bpy)^{3+}$ with the transilluminator is shown in Figure 3. Despite slightly greater DNA light damage using this alternative light source, the footprinted region again spans 10 base pairs (64−73), which is in excellent agreement with results obtained using the Hg/Xe lamp. It is noteworthy that some hyperreactivity by the rhodium complex is evident within the binding site in the absence of protein (lane F), and this reactivity, though reduced, is still present to some extent in the presence of protein (position 66, lane F and G). Nonetheless, densitometer scanning and subtraction of light controls yields footprints of equally high resolution to those obtained with a high power lamp.

Establishment of Optimal Conditions for Cleavage by $Rh(phi)_2(bpy)^{3+}$

In order to establish the effect of different reaction conditions on the sequence-neutrality and intensity of $Rh(phi)_2(bpy)^{3+}$ cleavage, a series of experiments to characterize the cleavage were also conducted. The effect of varying the rhodium/base pair ratio is shown in Figure 4 (lanes I−K and O), together with the effect of irradiation time (lanes F−H and L−N) and irradiation power (lanes J and R−V). As the Rh/DNA ratio decreases, cleavage by the complex shows increasing sequence selectivity. Although no clear consensus sequence is evident, sequences such as 5′-TATG-3′ (51−48 and 37−34 bp) as well as, more generally, alternating purine-pyrimidine sequences are cleaved more strongly relative to background at low concentrations of $Rh(phi)_2(bpy)^{3+}$. DNA cleavage by the complex at such alternating sequences is still efficient at rhodium concentrations as low as 50 nM and reflects a preference of the metal complex for these sequences. Cleavage at pyrimidine bases is slightly more efficient than at purine bases. At rhodium/base pair ratios of $\geq$ 0.5, however, the cleavage reaction is almost completely sequence neutral, and certainly random enough for purposes of footprinting.

Unlike the effect of varying the rhodium/base pair ratio, differences in irradiation time or power do not cause changes in cleavage specificity of the metal complex. As can be seen from Figure 4, changes in irradiation time or power are roughly proportional to the extent of cleavage. Varying the wavelength of irradiation also causes only little change in cleavage pattern. Shorter-wavelength light (300−320 nm) is much more efficient for activating $Rh(phi)_2(bpy)^{3+}$ than is longer-wavelength light (340−365 nm). It is impractical to use light below 310 nm, however, because photodamage in the absence of the rhodium complex occurs, which introduces background noise.

Figure 5 Effect of metal ions, EDTA, and glycerol on DNA photocleavage by $Rh(phi)_2(bpy)^{3+}$. Lanes A, B, and C: Intact DNA, dark control, and light control, respectively. Lanes D and E: Maxam-Gilbert A+G and T+C reactions, respectively. Lane F: cleavage by $Rh(phi)_2(bpy)^{3+}$ in the absence of additives. Lanes G, H, and I: in the presence of additional 0.1, 0.5, and 2.5 M NaCl, respectively. J, K, and L: In the presence of 1, 10, and 100 mM $MgCl_2$. M, N, and O: in the presence of 1, 10, and 100 mM $CaCl_2$, . P, Q, and R: in the presence of 1, 10 , and 50 mM EDTA. S, T, and U: in the presence of 0.1, 1, and 10 % of glycerol. Fragment was 3′-end-labeled and irradiation time was 5 min with a Hg/Xe lamp under the standard conditions described for $Rh(phi)_2(bpy)^{3+}$ photocleavage.

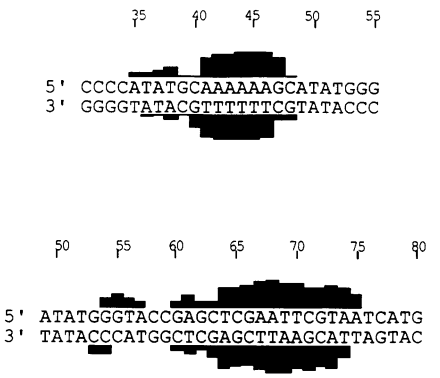

Figure 6 Sequence of the regions of interest on the 245 base pair restriction fragment used in these experiments showing in histogram form the footprinted sites both for distamycin (above) and EcoRI (below) using $Rh(phi)_2(bpy)^{3+}$. The 5'-end-labeled fragment is labeled with ^{32}P on the 5'-end of the upper strand and the 3'-end-labeled fragment is labeled with ^{32}P at the 3'-end of the lower strand.

The effect of different buffers on the cleavage reaction was also examined at pH 7 (data not shown). No changes in specificity or intensity of the cleavage reaction are observed in any of the following buffers at pH 7: (1) 50 mM sodium cacodylate(-HCl), (2) 50 mM potassium phosphate, (3) 50 mM Tris(-HCl), and (4) 50 mM Tris(-HCl), 20mM sodium acetate, and 18 mM sodium chloride. When the reaction is carried out at pH 6 (50 mM sodium cacodylate buffer) or pH 8 (50 mM Tris(-HCl) buffer), there are few detectable differences in the $Rh(phi)_2(bpy)^{3+}$ cleavage pattern. Sequence-neutrality of the photocleavage reaction is also unaffected by the temperature of incubation varied from 0° C to 37° C.

Effect of Commonly Used Biochemical Reagents on Cleavage by $Rh(phi)_2(bpy)^{3+}$

The effect of various salts (NaCl, $MgCl_2$, $CaCl_2$) on the photocleavage reaction is shown in Figure 5 (lanes F−O). The photocleavage reaction is not inhibited in 100 mM NaCl, 10 mM $MgCl_2$, or 10 mM $CaCl_2$, salt concentrations necessary for *in vivo* applications and sometimes required with particular DNA-binding proteins. At higher concentrations of these salts, some sequence preferences (for alternating pyrimidine-purine segments) appear which are identical to those observed at low $Rh(phi)_2(bpy)^{3+}$ concentration, consistent with a decrease in binding affinity at very high salt concentrations. Cleavage is not altered in the presence of 1 mM EDTA, although some GC selectivity is apparent in the presence of 10−100 mM EDTA (Figure 5 lanes P−R). Dithiothreitol at concentrations of 1mM or higher causes only slight changes in relative band intensities while another reducing agent, 3-mercaptopropionic acid, has no effect up to 10 mM (data not shown). Bovine serum albumin (60 μg/ml) or 10 % glycerol (Figure 5 lanes S−U) has no affect on photocleavage by $Rh(phi)_2(bpy)^{3+}$.

DISCUSSION

Figure 6 summarizes the footprinting results using $Rh(phi)_2(bpy)^{3+}$ at both the distamycin and EcoRI binding sites on the restriction fragment examined. It is apparent that $Rh(phi)_2(bpy)^{3+}$ produces well defined, highly resolved footprints of both a small peptide binding in the minor groove and a large DNA-binding protein. The binding sites delineated

by the rhodium footprints both for distamycin and EcoRI are in excellent agreement with the crystallographic data for these DNA-binding molecules in cocrystals with oligonucleotides (24,25). The crystal structures indicate that distamycin and EcoRI having binding site sizes of six and ten, respectively. The footprints obtained with $Rh(phi)_2(bpy)^{3+}$ therefore are among the most precise observed thus far using footprinting methodology. Importantly the resolution is maintained even when $Rh(phi)_2(bpy)^{3+}$ is photoactivated using a simple transilluminator, making this technique accessible to almost any molecular biology laboratory.

There are several features of the photocleavage reaction promoted by $Rh(phi)_2(bpy)^{3+}$ which contribute to the resolution and clarity of its footprints. The first important characteristic for any successful footprinting reagent is the sequence neutrality in its cleavage. $Rh(phi)_2(bpy)^{3+}$ cleaves DNA quite uniformly; some sequence selectivity is apparent with the reagent only at nanomolar concentrations. Since cleavage is obtained at all nucleotides, single-nucleotide footprinting resolution is possible. Two interrelated features likely to be important in achieving the sharpness of the rhodium footprint are the rigidity of the complex and its apparent lack of a diffusing species to mediate the cleavage reaction. Mechanistic studies of phi complexes of rhodium(III) currently in progress in our laboratory suggest that cleavage occurs as a result of a direct hydrogen abstraction from the sugar by a ligand radical generated by photolysis. On high resolution gels, the cleaved fragments, with 5′-phosphate and 3′-phosphate termini, comigrate with Maxam-Gilbert reactions. Cleavage reactions with $Rh(phen)_2phi^{3+}$, a close analogue which shows some sequence selectivity, furthermore reveals single nucleotide cuts rather than a distribution of cuts at each binding site as is common with reagents that cleave DNA in reactions mediated by hydroxyl radicals (26) or singlet oxygen (27). The sharpness in footprint with $Rh(phi)_2(bpy)^{3+}$ may then result from the fact that the rigid rhodium complex can occupy and cleave directly at all sites that are not obstructed by the DNA binding agent and cannot cleave directly or indirectly within the obstructed region since the reagent does not cleave through a diffusible intermediate and lacks a floppy appendage which itself contains the cleaving functionality. The footprint with $Rh(phi)_2(bpy)^{3+}$ is, then, inherently 'all or none', producing a high contrast image. The pattern of cleavage obtained would contrast that found with $Fe(EDTA)^{2-}$, for example, which is mediated by hydroxyl radicals. With $Fe(EDTA)^{2-}$, information has been obtained regarding subtle structural details associated with how domains within a DNA-binding protein associate with the helix rather than the edges of the protein binding site. $Rh(phi)_2(bpy)^{3+}$ is not likely to be useful for such experiments. Instead the complex is extremely sensitive in sharply delineating the boundaries of a protein binding site with high contrast.

Another important aspect contributing to the versatility of $Rh(phi)_2(bpy)^{3+}$ as a footprinting reagent is the fact that the complex appears to bind to the helix by intercalation. Although a crystal structure is lacking on the phi complexes bound to oligonucleotides, helix unwinding results on a series of ruthenium complexes containing the phi ligand (28) as well as on $Rh(phi)_2(bpy)^{3+}$ itself (29) indicate helix unwinding angles that are comparable to ethidium. Intercalative binding by a footprinting reagent increases the range of applicability for the reagent, since intercalators can sense binding molecules in both the major and minor grooves. An intercalative interaction requires local helical unwinding and proteins bound to the one face of a helix clamp it shut against intercalation from the other side. Groove binding agents, in contrast, can sense only those molecules which bind in the same groove, unless binding to the other groove causes an appreciable structural

alteration. Hydroxyl radical cleavage generated by $Fe(EDTA)^{2-}$, which does not bind to the helix itself, apparently reacts preferentially with minor groove protons, leading to a substantial weighting in footprints to those structural perturbations which occur in the minor groove. Since an intercalator can sense binding molecules in either groove, it becomes of secondary importance whether the intercalator itself binds from either the minor or major groove. Based upon analogy to other phi complexes of rhodium(III) as well as upon results with other metallointercalating agents, it is possible that this footprinting reagent is also unique in binding from the major groove (17, 30). It should be noted in this context that the distamycin footprint with $Rh(phi)_2(bpy)^{3+}$ shows a single nucleotide shift to the 3′ side in the protection pattern and no pattern asymmetry is clearly apparent in the EcoRI footprint. For the distamycin binding site, other footprinting reagents which appear to bind from the minor groove have shown 3′-shifts with a larger magnitude (2−3 nucleotides) (9, 31).

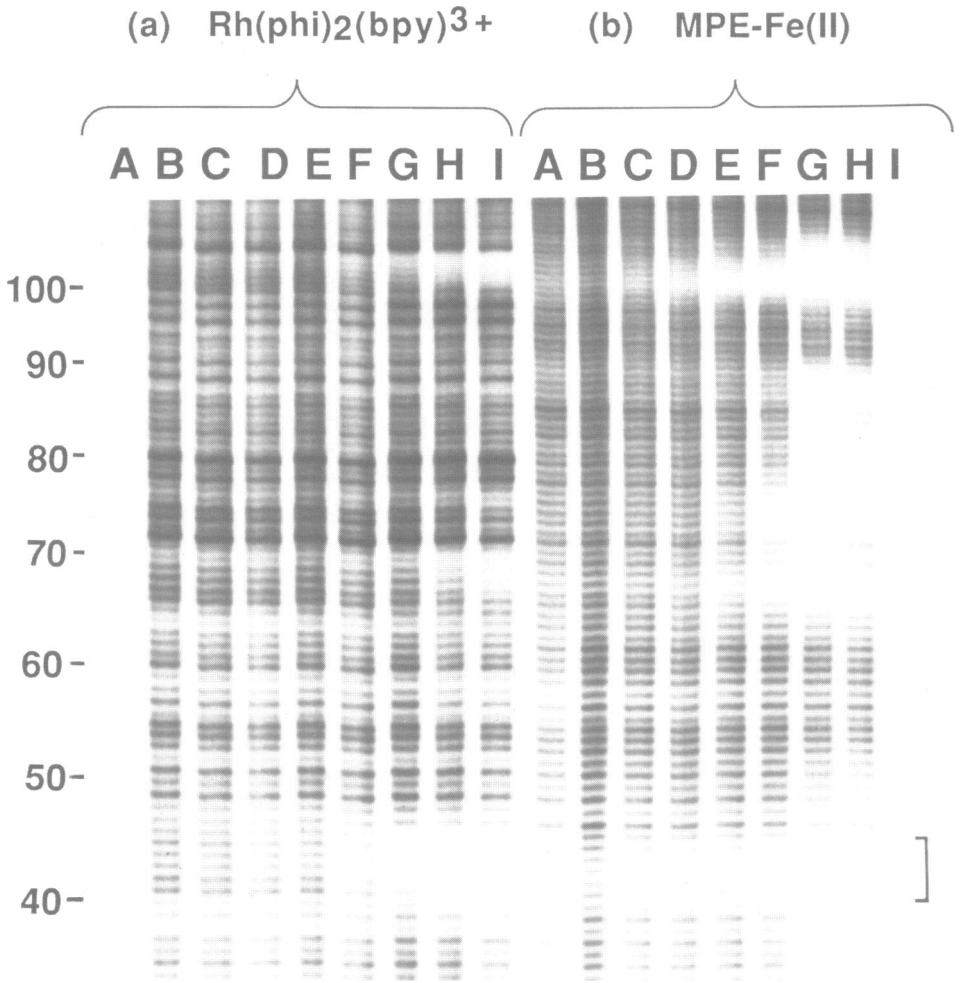

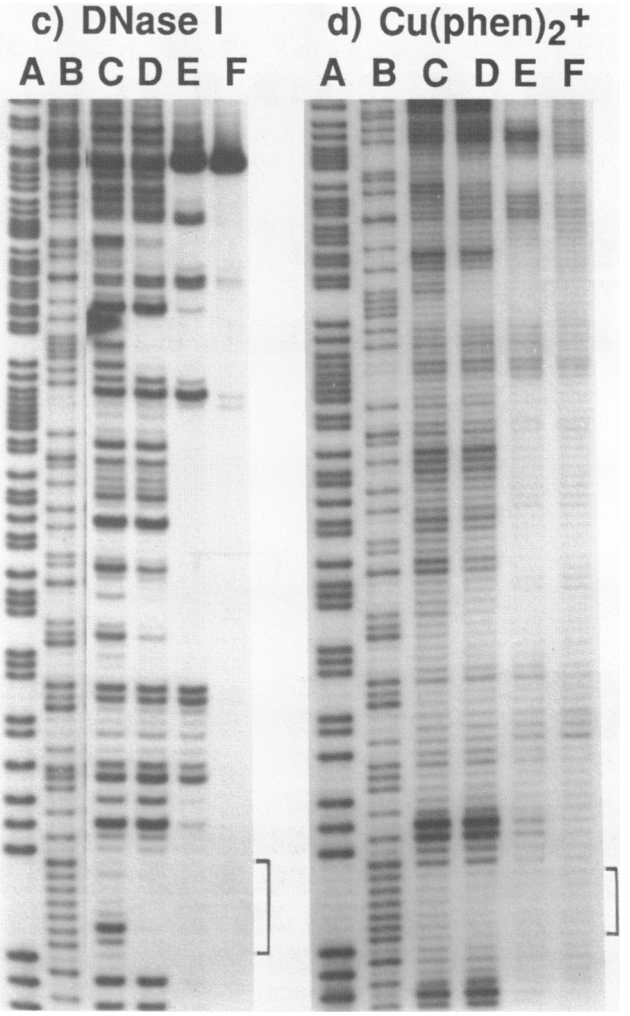

Figure 7 Comparison of distamycin footprinting by $Rh(phi)_2(bpy)^{3+}$ (**a**), MPE-Fe(II) (**b**), DNase I (**c**), and $Cu(phen)_2^+$ (**d**). Footprinted regions of the T_6 tract are indicated by brackets. The 3′-end-labeled fragment, with 25 μMbp total DNA, and 12.5 μM metal complexes (Rh, Fe, and Cu) were used. For better resolution of the footprints, the higher molecular weight region of the gels are not shown.

(**a**) Lane A: Light control. Lane B: In the absence of distamycin. Lanes C−I: in the presence of 0.125, 0.25, 0.50, 1.25, 2.5, 5.0, and 12.5 μM distamycin, respectively. Irradiation time was 7 min.

(**b**) Lane A: In the absence of distamycin. Lanes B−H: in the presence of 0.125, 0.25, 0.50, 1.25, 2.5, 5.0, and 12.5 μM distamycin, respectively. I: in the absence of MPE. Incubation for DNA cleavage reaction was 5 min at 37 °C.

(**c**) Lanes A and B: Maxam-Gilbert A+G and T+C reactions, respectively. Lane C: In the absence of distamycin; D, E, and F: in the presence of 1.25, 5.0, and 25 μM distamycin, respectively. Incubation was 5 min at 37 °C in the presence of 0.2 units DNase I. The bracket indicates the footprint from 40−47.

(**d**) Lanes A and B: Maxam-Gilbert A+G and T+C reactions, respectively. Lane C: In the absence of distamycin. Lanes D, E, and F: in the presence of 1.25, 5.0, and 25 μM distamycin, respectively. Incubation was 13 sec at 37 °C. The bracket indicates the footprint from 41−46.

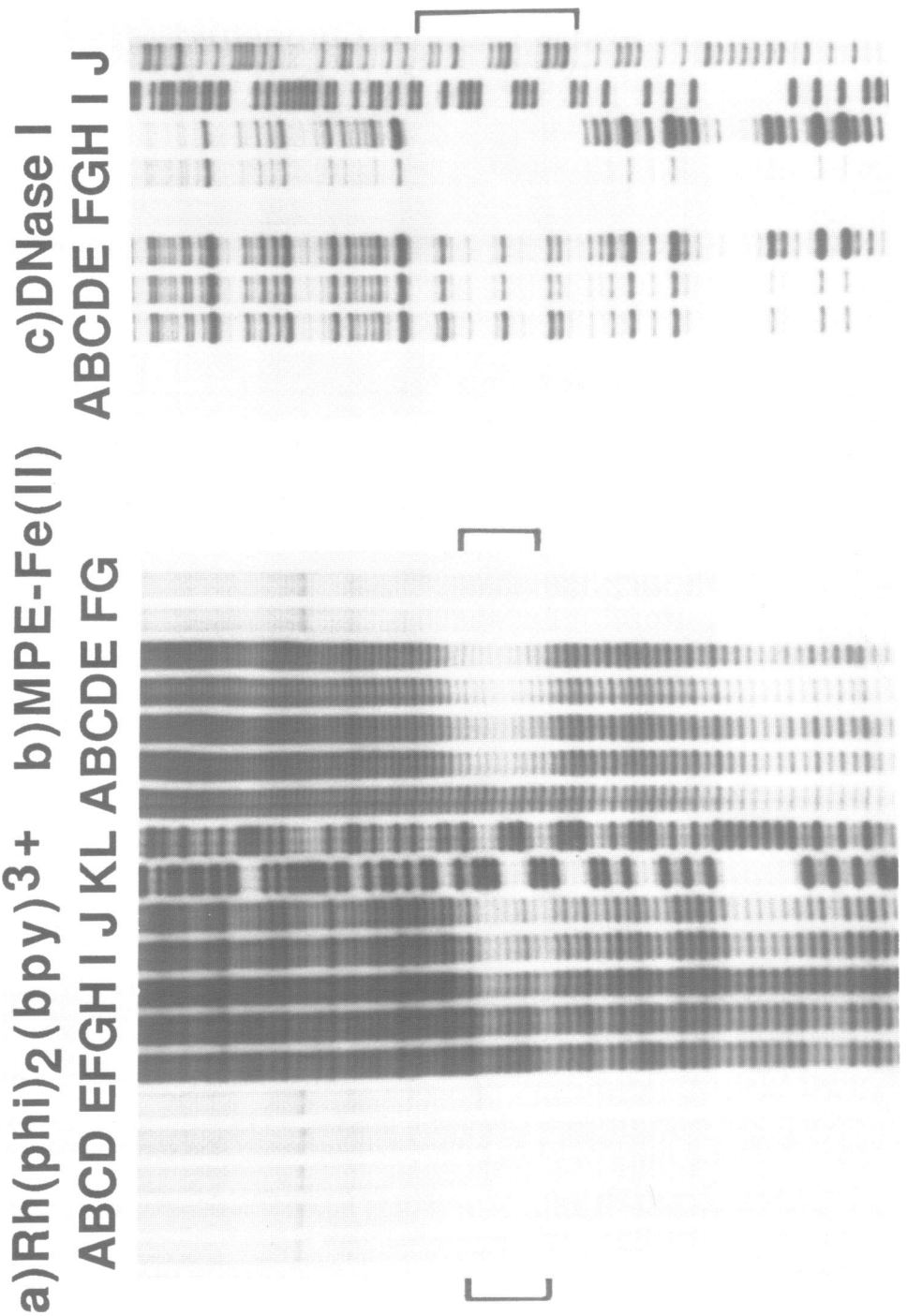
a)Rh(phi)2(bpy)3+
ABCD EFGH I J KL
b)MPE-Fe(II)
ABCDE FG
c)DNase I
ABCDE FGH I J

Comparisons in footprinting of distamycin are made in Figure 7 between $Rh(phi)_2(bpy)^{3+}$and other popular footprinting reagents, MPE-Fe(II), DNase I and $Cu(phen)_2^+$. Comparative footprinting of EcoRI is shown in Figure 8, although $Cu(phen)_2^+$ could not be included as it failed to footprint the protein in our hands (and also in the literature (22)). This result is not surprising given that the copper complex likely binds without intercalating in the minor groove. DNase I footprints yield an exaggerated ligand site size, with distamycin and EcoRI, due to both the sequence selectivity and large size of the enzyme. $Cu(phen)_2^+$ is a small reagent which could conceivably footprint distamycin to high resolution. However, as is apparent in Figure 7d, $Cu(phen)_2^+$ lacks the necessary sequence neutrality.

The footprinting reagent most similar to $Rh(phi)_2(bpy)^{3+}$ in resolution and sequence-neutrality is MPE-Fe(II). As shown in Figures 7b and 8b, clear footprints of distamycin and EcoRI are obtained with this reagent. The sequence neutrality in reactions with MPE-Fe(II) may be somewhat higher than that with the rhodium complex. The footprinting pattern with MPE-Fe(II) is also of comparable resolution to that found with $Rh(phi)_2(bpy)^{3+}$ but may not be as sharp as is seen with the rhodium complex, likely because the reaction is mediated by a diffusible species. Another notable difference between $Rh(phi)_2(bpy)^{3+}$ and MPE-Fe(II) is that the latter shows a greater propensity to detect weak distamycin binding sites at comparable concentrations. This is probably a result of the lower binding constant of MPE-Fe(II) to DNA [1.5×10^5 M^{-1} for MPE-Ni(II)] (9). One can also derive the binding constant for $Rh(phi)_2(bpy)^{3+}$ to the distamycin binding site based upon competition (32), and such an analysis yields an apparent $Rh(phi)_2(bpy)^{3+}$ binding constant to the A_6 site of 10^6-10^7 M^{-1}. This calculation is also consistent with the observation that DNA (5 μM bp) can be efficiently cleaved by $Rh(phi)_2(bpy)^{3+}$ at concentrations of 50 nM. Taken together, the binding data indicate that $Rh(phi)_2(bpy)^{3+}$ has a higher association constant than MPE-Fe(II) to B-DNA. Since both reagents bind less avidly to DNA than does EcoRI to its recognition site, both reagents show a more comparable footprinting pattern for the protein.

Besides the quality of its footprints, an important practical advantage in using $Rh(phi)_2(bpy)^{3+}$ for footprinting is simply its ease and range of handling. The complex is stable indefinitely in the solid state or stored as a frozen aqueous solution. It is not inhibited by moderate concentrations of divalent cations, EDTA, reducing agents, or glycerol. No

Figure 8 Comparison of $Rh(phi)_2(bpy)^{3+}$ footprinting of EcoRI (**a**) with other footprinting techniques, MPE-Fe(II) (**b**) and DNase I (**c**). Footprinted regions are indicated by brackets at 64–73 for $Rh(phi)_2bpy^{3+}$ and MPE-Fe(II) and 59–76 for DNAse. 3'-end-labeled fragment, 5μM bp total DNA, and 5μM metal (Rh or Fe) were employed.

(a) Lane A: Intact DNA fragment. Lanes B and C: Dark control in the absence and presence (200 units) of *Eco*RI, respectively. Lanes D and E: Light control in the absence and presence (200 units) of *Eco*RI. Lane F: In the absence of *Eco*RI. Lanes G–J: In the presence of 50, 100, 200, and 300 units of *Eco*RI, respectively; Irradiation time was 5 min with a Hg/Xe lamp. Lanes K and L: Maxam-Gilbert A+G and T+C reactions.

(b) Lane A: In the absence of *Eco*RI. Lanes B–E: In the presence of 50, 100, 200, and 300 units of *Eco*RI, respectively. Lanes F and G: DNA controls in the absence of MPE or Fe(II), respectively. Lanes K and L: Maxam-Gilbert A+G and T+C reactions. Samples were incubated at 37 °C for 5 min.

(c) Lanes A and B: DNA in the absence of *Eco*RI and DNase 1. Lane C: In the absence of *Eco*RI and in the presence of 0.2 units DNase I incubated at 37 °C for 2 min. Lanes D and E: In the presence of 64 units *Eco*RI and in the presence of 0.2 units DNase I incubated at 37 °C for 2 and 10 min, respectively. Lanes F, G, and H: In the presence of 252 units *Eco*RI and in the presence of 0.2, 0.8, and 1.6 units DNase I, respectively, incubated at 37 °C for 2, 10, and 10 min, respectively. Lanes I and J: Maxam-Gilbert A+G and T+C, reactions respectively.

complicated procedures or highly reactive species are required for the cleavage reaction, and clear footprinting may be obtained over a wide range of ligand and $Rh(phi)_2(bpy)^{3+}$ concentrations. These characteristics contrast $Rh(phi)_2(bpy)^{3+}$ with reagents that require chemical activation such as $Cu(phen)_2^+$ and MPE-Fe(II).

In summary, photoactivated cleavage with $Rh(phi)_2(bpy)^{3+}$ permits high sensitivity, clear resolution, wide applicability and excellent control in footprinting experiments of DNA-binding molecules. Since $Rh(phi)_2(bpy)^{3+}$ can be used with common UV light sources, the requirement for photolysis should be an advantage rather than an inconvenience. Perhaps most importantly, photofootprinting reagents such as $Rh(phi)_2(bpy)^{3+}$ may lend themselves especially well to footprinting DNA-bound proteins within living cells.

ACKNOWLEDGEMENTS

K.U. conducted this research as a Fulbright Fellow. We are grateful also to the National Institute of General Medical Science (GM33309 to J.K.B.; National Research Service Training Award for A.M.P., GM07216), to the National Foundation for Cancer Research, and to Bethesda Research Laboratories fo their financial support.

*To whom correspondence should be addressed

Present addresses: +Pharmaceutical Institute, Tohoku University, Aobayama, Sendai 980, Japan, §Department of Chemistry and Biochemistry, University of Colorado, Boulder, CO 80309 and ΦDivision of Chemistry and Chemical Engineering, California Institute of Technology, Pasedena, CA 91125, USA

REFERENCES

1. Galas, D.J. and Schmitz, A. (1978) *Nucl. Acids Res.* **5**, 3157–3170.
2. Dervan, P.B. (1986) *Science* **232**, 464–471.
3. Tullius, T.D. (1987) *Trends Biochem. Sci.* **12**, 297–300.
4. Sigman, D.S. (1986) *Accts. Chem. Res.* **19**, 180–186.
5. Van Dyke, M.W., Roeder, R.G. and Sawadogo, M. (1988) *Science* **241**, 1335–1338. Kownin, P., Bateman, E.and Paule, M.R. (1987) *Cell* 50, 693–699.
6. Drew, H.R. and Travers, A.A. (1984) *Cell* 37, 491–502. Suggs, J.W. and Wagner, R.W. (1986) *Nucl. Acids Res.* **14**, 3703–3716. Suck, D., Lahm, A. and Oefner, C. (1988) *Nature* **332**, 464–468.
7. Jessee, B., Gargiulo, G., Razvi, F. and Worcel, A. (1982) *Nucl. Acids Res.* **10**, 5823–5834. Veal, J. M. and Rill, R. L. (1989) *Biochemistry* **28**, 3243–3250. Veal, J. M. and Rill, R. L. (1988) *Biochemistry* **27**, 1822–1827. Kobashi, K. (1968) *Biochim. Biophys. Acta* **158**, 239–245. Yoon, C., Kuwabara, M. D., Law, R., Wall, R. and Sigman, D. S. (1988) *J. Biol. Chem.* **263**, 8458–8463.
8. Ward, B., Skorobogaty, A. and Dabrowiak, J.C. (1986) *Biochemistry* **25**, 6875–6883. Ward, B., Skorobogaty, A. and Dabrowiak, J. C. (1986) *Biochemistry* **25**, 7827–7833.Dabrowiak, J. C., Ward, B. and Goodisman, J. (1989) *Biochemistry* **28**, 3314–3322. Ward, B., Rehfuss, R., Goodisman, J. and Dabrowiak, J. C. (1988) *Biochemistry* **27**, 1198–1205.
9. Van Dyke, M.W., Hertzberg, R.P. and Dervan, P.B. (1982) *Proc. Natl. Acad. Sci. USA* 79, 5470–5474. Hertzberg, R. P. and Dervan, P. B. (1982) *J. Am. Chem. Soc.* 104, 313–315. Hertzberg, R. P. and Dervan, P. B. (1984) *Biochemistry* **23**, 3934–3945.
10. Van Dyke, M.W.and Dervan, P.B. (1983) *Nucl. Acids Res.* **11**, 5555–5567.
11. Hurley, L.H., Lee, C.-S., McGovren, J.P., Warpehoski, M.A., Mitchell, M.A., Kelly, R.C. and Aristoff, P.A. (1988) *Biochemistry* **27**, 3886–3892.
12. Cartwright, I.L. and Elgin, S.C.R. (1986) *Mol. Cell. Biol.* **6**, 779–791. Gunderson, S.I., Chapman, K.A. and Burgess, R.R. (1987) *Biochemistry* **26**, 1539–1546. Pruijn, G.J.M., van Miltenburg, R.T., Claessens, J.A.J. and van der Vliet, P.C. (1988) *J. Virology* **62**, 3092–3102.
13. Tullius, T.D., Dombrowski, B.A., Churchill, M.E.A. and Kam, L. (1987) *Methods in Enzymology* 155, 537–558. Tullius, T. D. and Dombroski, B. A. (1986) *Proc. Natl. Acad. Sci. USA* 83, 5469–5473.
14. Becker, M. M., and Wang, J. C. (1984) *Nature* **309**, 682–687. Becker, M. M., Lesser, D., Kurpiewski, M., Baranger, A. and Jen-Jacobson, L. (1988) *Proc. Natl. Acad. Sci. USA* **85**, 6247–6251. Selleck, S.

B. and Majors, J. (1988) *Proc. Natl. Acad. Sci. USA* 85, 5399–5403. Wang, Z., and Becker, M. M. (1988) *Proc. Natl. Acad. Sci. USA* **85**, 654–658.
15. Nielsen, P.E., Jeppesen, C. and Buchardt, O. (1988) *FEBS Lett.* **235**, 122–124. Jeppesen, C. and Nielsen, P.E. (1989) *Nucl. Acids Res.* **17**, 4947.
16. Jeppesen, C., Buchardt, O., Henriksen, U., and Nielsen, P. E. (1988) *Nucl. Acids Res.* **16**, 5755–5770. Zhen, W.-P., Jeppesen, C. and Nielsen, P. E. (1988) *FEBS Lett.* **229**, 73–76.
17. Pyle, A.M., Long, E.C. and Barton, J.K. (1989) *J. Am. Chem. Soc.* **111**, 4520–4522.
18. Fox, K.R. (1988) *Biochem. Biophys. Res. Comm.* **155**, 779–785.
19. Maniatis,T., Fritsch, E.F. and Sambrook, J. (1982) *Molecular Cloning, a Laboratory Manual, Cold Spring Harbor Laboratory, Cold Spring Harbor, N.Y.*
20. Luck, G., Zimmer, C., Reinert, K.-E., and Arcamone, F. (1977) *Nucl. Acids Res.*4, 2655–2670.
21. Modrich, P., and Zabel, D. (1976) *J. Biol. Chem.* 251, 5866–5874.
22. Fox, K. R. and Waring, M. J. (1984) *Nucl. Acids Res.* **12**, 9271–9285. Spassky, A, and Sigman, D. S. (1985) Biochemistry **24**, 8050–8056. Kuwabara, M., Yoon, C., Goyne, T., Thederahn, T. and Sigman, D.S. (1986) *Biochemistry* **25**, 7401–7408.
23. Maxam, A. and Gilbert, W. (1980) *Methods in Enzymology* **65**, 499–560.
24. Coll, M., Frederick, C.A., Wang, A. H.-J., Rich, A. (1987) *Proc. Natl. Acad. Sci. USA* **84**, 8385–8389. Kopka, M.L., Yoon, C., Goodsell, D., Pjura, P. and Dickerson, R.E. (1985) *J. Mol. Biol.* **183**, 553–563.
25. Frederick, C.A., Grable, J., Melia, M., Samudzi, C., Jen-Jacobson, L., Wang, B.-C., Greene, P., Boyer, H.W., Rosenberg, J.M. (1984) *Nature* 309, 327–331. McClarin, J. A., Frederick, C. A., Wang, B.-C., Greene, P., Boyer, H. W., Grable, J., and Rosenberg, J. M. (1986) *Science* **234**, 1526–1541.
26. Sluka, J.P., Horvath, S.J., Bruist, M.F., Simon, M.I. and Dervan, P.B. (1987) *Science* 238, 1129–1132.
27. Mei, H.-Y. and Barton, J.K. (1988) *Proc. Natl. Acad. Sci. USA* 85, 1339–1343.
28. Pyle, A.M., Rehmann, J.P., Meshoyrer, R., Kumar, C.V., Turro, N.J. and Barton, J.K. (1989) *J. Am. Chem. Soc.* **111**, 3051–3058.
29. Pyle, A.M. (1989) Ph.D. Dissertation, Columbia University.
30. It appears that, in general, metallointercalation reagents associate from the major groove of the DNA helix. For an example, see: Wang, A. H.-J., Nathans, J., van der Marel, B., van Boom, J.H., Rich, A. (1978) *Nature* **276**, 471–474.
31. Portugal, J., & Waring, M. J. (1987) *FEBS Lett.* **225**, 195–200. Van Dyke, M. W., Hertzberg, R. P. and Dervan, P. B. (1982) *Proc. Natl. Acad. Sci. USA* 79, 5470–5474. Harshman, K. D. and Dervan, P. B. (1985) *Nucl. Acids Res.* **13**, 4825–4835.
32. Given that the K_b of distamycin to the T_6 footprinting site is $\sim 10^{7-8} M^{-1}$ (Zimmer, C. and Waehnert, U. (1986) *Prog. Biophys. Molec. Biol.* **47**, 31–112.) and given the concentrations of the rhodium complex and distamycin used in the experiment, one can apply a competitive model similar to that in Segel, I.H. (1975) *Enzyme Kinetics: Behavior and Analysis of Rapid Equilibrium and Steady State Enzyme Systems*, Wiley Interscience, New York.

This article, submitted on disc, has been automatically converted into this typeset format by the publisher.